

固化对水性环氧粘结固体 润滑涂层理化及摩擦学性能的影响

王月梅^{1,2}, 周惠娣¹, 陈建敏¹, 陈磊¹, 冶银平¹

1. 中国科学院兰州化学物理研究所固体润滑国家重点实验室, 甘肃 兰州 730000;
2. 中国科学院研究生院, 北京 100049)

[摘要] 为了确定水性环氧粘结固体润滑涂层的最佳固化条件, 采用 MFT-R 4000 型往复摩擦磨损试验机评价了不同固化条件对其摩擦学性能的影响, 用傅立叶变换红外光谱 (FTIR) 和示差扫描量热法 (DSC) 表征手段, 确定了体系的最佳固化条件。结果表明: 固化条件不同, 涂层的摩擦学性能差异很大; 水性粘结剂与水性固化剂的最佳质量比为 2 : 1, 最佳固化温度为 75 °C, 最佳固化时间为 2 h; 以最佳条件制备的水性环氧粘结固体润滑涂层具有优异的理化性能和摩擦学性能, 摩擦磨损寿命比传统的有机溶剂型粘结固体润滑涂层约长 30%。本研究为制备高性能环保型粘结固体润滑涂层提供了可能。

[关键词] 固体润滑涂层; 水性环氧树脂; 粘结固体润滑剂; 固化条件; 摩擦学性能

[中图分类号] TQ323.5; TH117.3 **[文献标识码]** A **[文章编号]** 1001-1560(2010)11-0007-03

0 前言

水性环氧粘结固体润滑剂^[1,2]以水性环氧涂料^[3-6]为粘结剂, 二硫化钼、石墨等为润滑填料, 水为分散介质, 不含挥发性有机化合物 (VOC), 价格低廉、无气味、不燃、环保等。目前, 大多的研究集中在溶剂型固体润滑剂^[7-9], 对水性环氧粘结固体润滑剂的研究只有少数的专利^[1,2]。水性润滑剂代表着未来的发展方向。

然而, 在水性粘结固体润滑剂的固化过程中, 粘结剂 (即水性环氧树脂涂料) 容易产生核壳结构, 导致固化不完全, 致使涂层性能变差^[10-12]; 而且与润滑剂的搅拌混合, 也会使其固化性能受到一定的影响。因此, 最佳固化条件的确定对于开发高性能的水性粘结固体润滑涂层具有重要的意义。本工作制备了水性 MoS₂ 粘接润滑涂层, 采用自制的往复摩擦磨损试验机评价了不同固化条件对水性环氧粘结固体润滑剂摩擦

学性能的影响; 以现代表征技术研究了水性环氧粘结固体润滑涂层的最佳固化条件; 进一步考察了水性环氧树脂粘结固体润滑涂层最佳固化条件下的理化性能和摩擦学性能, 以期制备高性能环保型粘结固体润滑涂层提供可能。

1 试验

1.1 涂层制备

基材处理: 基材材料是 45 钢和 马口铁, 尺寸均为 12.7 mm × 12.7 mm × 19.0 mm; 作常规喷砂、丙酮超声等处理, 除去锈、油。

水性粘结固体润滑涂料配制: 将 25.0% 固体润滑剂 (二硫化钼, 固含量 99%)、0.5% 表面活性剂 (聚乙二醇) 和水球磨 48 h; 加入一定量的粘结剂 (乳白色水性环氧树脂乳液, 固含量 50%) 和固化剂 (水性黄色黏稠液聚酰胺, 固含量 60%) (两者质量比为 1.0 : 4.2), 搅拌均匀。

水性环氧粘接固体润滑涂层喷涂: 以 0.15 ~ 0.20 MPa 压缩氮气作驱动气体, 将配制好的涂料喷涂到基材表面; 以不同温度进行固化, 得到水性 MoS₂ 粘接润滑涂层, 厚度为 (20 ± 2) μm。

1.2 涂层表征

采用 MFT-R 4000 型往复摩擦磨损试验机评价涂

[收稿日期] 2010-06-10

[基金项目] 国家自然科学基金委创新研究群体科学基金 (50421502); 国家 973 计划 (2007CB607601) 资助

[通信作者] 周惠娣 (1965-), 研究员, 硕士生导师, 主要从事摩擦学与表面工程方面的研究, 电话 0931-4968138, E-mail: hdzhou@lzb.ac.cn

层的摩擦学性能:上试样为 AISI 440C 钢球, $\phi 12.00$ mm, 硬度 58 HRC, 下试样为具有涂层的 45 钢, 两者为点接触; 施加的载荷为 30 N, 摩擦长度 2.5 mm, 频率 10 Hz, 温度 24 ~30 °C, 空气相对湿度 30% ~50%。

采用 IFS66V/S 型红外光谱仪 (FTIR) 测试涂层固化后环氧特征峰的变化: 将马口铁上的固化涂层用刀片刮下, 用 KBr 粉末压片后进行红外测试。

采用 STA 449C 同步热分析仪 (DSC) 测试涂层的最佳固化温度; 预先将待测试样真空干燥 (室温, 真空度 0.07 MPa) 0.5 h, 除去水分; 每次约取 5 mg, 分别以 5, 10, 15 °C/min 升温速率进行测试 (以空气作吹扫气, 氮气作保护气)。

分别按 GB 1720 - 89, GB/T 1732 - 93 和 GB 1731 - 89 测试涂层的附着力、耐冲击性和柔韧性^[13]。

2 结果与讨论

2.1 水性粘接剂和水性固化剂最佳配比

5 种水性粘接剂和水性固化剂配比 100 °C 固化涂层的摩擦磨损性能见图 1 和图 2。

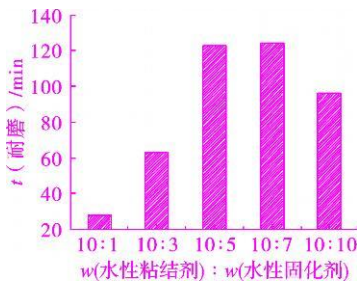


图 1 不同配比下水性 MoS₂ 粘结润滑涂层的耐磨寿命

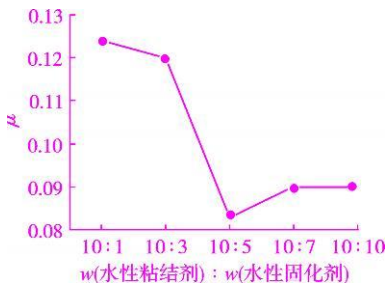


图 2 不同配比下水性 MoS₂ 粘结润滑涂层的摩擦系数

从图 1, 图 2 可以看出, 两者的配比不同, 涂层的摩擦学性能明显不同: 当配比为 10 : 5 时, 涂层的耐磨寿命 (磨穿某一厚度涂层所用时间) 较长、摩擦系数最低; 配比大于 10 : 7 或者小于 10 : 5 时, 涂层的耐磨寿命明显降低。因为涂层的耐磨性与粘接剂的固化程度直接相关, 固化程度越高, 交联密度越大, 耐磨性就越好, 当水性粘接剂与水性固化剂配比为 10 : 5 时, 涂层就

完全固化。

涂层的固化交联程度见图 3。

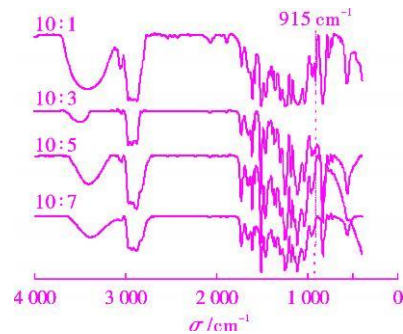
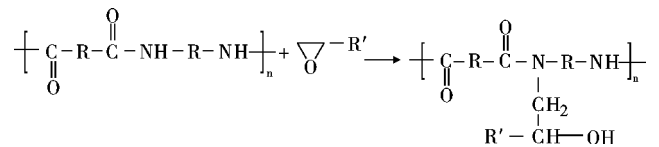


图 3 4 种水性粘接剂与水性固化剂配比时涂层的红外光谱

从图 3 可以看出: 1 508 cm⁻¹ 处的强吸收峰为苯环特征吸收峰, 且不同的配比时保持不变, 说明苯环未参与固化反应; 915 cm⁻¹ 处涂层的环氧特征峰强度随配比不同发生了明显的变化, 配比为 10 : 1 时, 环氧特征峰较强, 说明固化后环氧基有剩余, 配比为 10 : 3 时, 环氧特征峰明显减弱, 配比为 10 : 5 时, 环氧特征峰消失, 环氧基完全与酰胺基发生如下反应:



涂层固化交联不完全, 会导致其耐磨性变差。结合涂层的红外谱 (图 3) 及耐磨性数据 (图 1) 可以看出, 当两者配比为 10 : 5 时, 水性 MoS₂ 粘结固体润滑涂层具有优异的摩擦学性能。

2.2 涂层最佳固化温度

选定水性粘接剂和水性固化剂的配比为 10 : 5, 去除水分后, 3 种升温速率对涂层固化的影响见图 4。由图 4 可以看出, 放热峰的峰值随升温速率的增加而升高。固化反应是放热反应, 反应越完全, 放出的热量越多。以峰值对升温速率作图, 外推升温速率为 0 °C/min 时^[14, 15], 峰值温度为 75 °C (见图 5), 即在接近于零升温速率下, 75 °C 时放出的热量最多, 固化反应最容易发生。因此, 最佳固化温度确定为 75 °C。

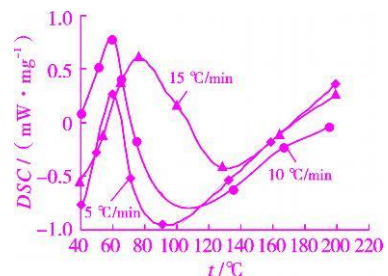


图 4 不同升温速率下涂层的 DSC 放热曲线

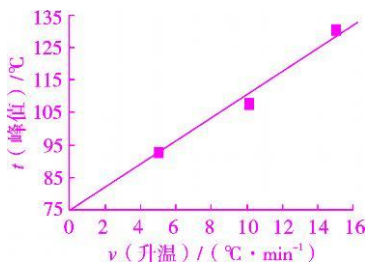


图5 峰值对升温速率的变化曲线

2.3 涂层最佳固化时间

选取上述优化条件,将涂层于室温下放置1 h后,75 $^{\circ}\text{C}$ 固化1,2,3 h,其耐磨结果见图6。从图6可以看出,固化1 h,耐磨寿命为80 min,固化2 h耐磨寿命增长至120 min,固化3 h和2 h相近,说明固化2 h,固化交联已比较完全。涂层不同时间固化后的红外光谱见图7;915 cm^{-1} 处室温放置1 h时涂层存在明显的环氧特征峰,环氧基没有完全参与反应,固化交联很不完全;75 $^{\circ}\text{C}$ 固化1 h后,存在微弱的环氧特征峰,其强度明显减弱,但仍有未反应的环氧基存在;固化2 h后,环氧峰完全消失,表明环氧基与酰胺基完全发生反应,固化交联完全。结合涂层的摩擦学和红外数据,确定最佳的固化时间为2 h。

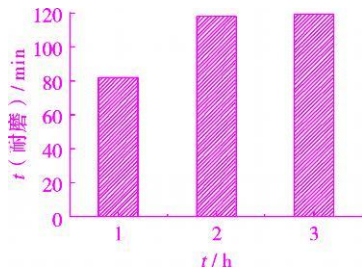


图6 不同时间固化后涂层的耐磨寿命

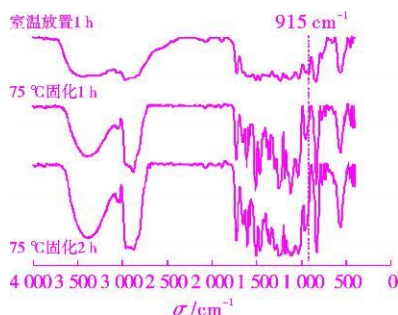


图7 不同时间固化后涂层的红外光谱

2.4 涂层理化性能和摩擦学性能

以最佳条件制备的涂层附着力为1级,抗冲击性能为60 cm,柔韧性为1 mm。这表明水性环氧树脂润滑涂层的理化性能可与有机溶剂型润滑涂层相媲美。

水性和有机溶剂型固体润滑涂层的摩擦学性能分

别见图8和图9(其中不同符号的曲线代表相同条件下3次重复试验的结果)。对比图8和图9可知:水性粘结固体润滑涂层的磨损寿命为400 min,比有机溶剂型的约长30%,摩擦系数平均值为0.068,比有机溶剂型的更低。这为开发高性能环保型的粘结固体润滑涂层提供了重要参考。

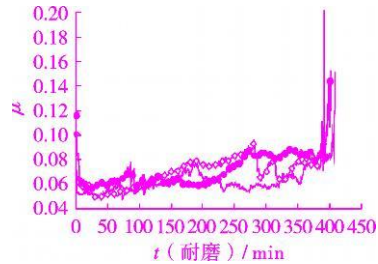


图8 水性粘结剂固体润滑涂层的摩擦曲线

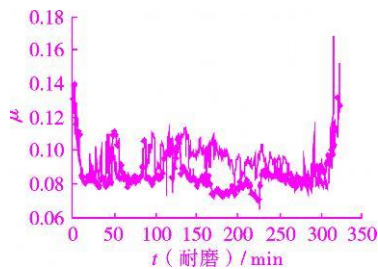


图9 有机型粘结剂固体润滑涂层的摩擦曲线

3 结论

(1)水性 MoS_2 粘结固体润滑涂层的最佳固化条件:水性粘接剂与水性固化剂的最佳配比为2:1,最佳固化温度为75 $^{\circ}\text{C}$,固化时间为2 h。

(2)以最佳固化条件制备的水性粘结固体润滑涂层主要含二硫化钼、石墨、三氧化二锑等,其理化性能优异,摩擦系数低、耐磨寿命长,优于有机溶剂型粘结固体润滑涂层。

[参 考 文 献]

- [1] Ikezawa, Atsushi, Yamaguchi, et al. Aqueous coating agent of hydrophilic resin, MoS_2 and Sb_2S_3 and/or Sb_2S_5 : US, 6538051[P]. 2003-03-25.
- [2] 李同生, 吕仁国, 刘旭军. 水性环氧粘结干膜润滑剂: 中国, 1450153A[P]. 2003-10-22.
- [3] 陈 钊, 施雪珍, 顾国芳. 双组分水性环氧树脂涂料[J]. 高分子通报, 2002(6): 63~70.
- [4] 陈立庄, 高延梅, 胡翔波, 等. 水分散型水性环氧涂料的制备[J]. 材料保护, 2005, 38(10): 51~53.
- [5] Jim D E, Derek S K, Pratap C K, et al. Waterborne epoxy protective coatings for metal [J]. Journal of Coatings Technology, 2002, 74(931): 63~73. (下转第13页)

- [4] Zhang W L, Frankel G S. Transition between pitting and intergranular corrosion in AA2024 [J]. *Electrochimica Acta*, 2003, 48 (9): 1 193 ~1 210.
- [5] Ruan S L, Frankel G S. Statistical Modeling of Minimum Intergranular Corrosion Path Length in High-Strength Aluminum Alloy [J]. *Technometrics* 2004, 46 (1): 69 ~75.
- [6] Samuels B W, Sotoudeh K, Foley R T. Inhibition and acceleration of aluminum corrosion [J]. *Corrosion*, 1981, 37 (2): 92 ~97.
- [7] Bellinger N C, Komorowski J P, Gould R W. Damage Tolerance Implications of Corrosion Pitting on Fuselage Lap Joints [J]. *Journal of Aircraft*, 1998, 35 (3): 487 ~491.
- [8] Jones R, Molent L. Study of multi-site damage of fuselage lap joints [J]. *Theoretical and Applied Fracture Mechanics* 1999, 32 (2): 81 ~100.
- [9] Kinzie R. Improved Corrosion Maintenance Practice [A]. The RTO AVI Specialists' Meeting on "Life Management Techniques for Aging Air Vehicles" [C]. Manchester: NATO, 2001: 8 ~11.
- [10] Zheng X. A novel model for crevice corrosion of lap joints [J]. *Corrosion*, 2001, 57 (7): 634 ~642.
- [11] Ferrer K S, Kelly R G. Development of an aircraft lap joint simulant environment [J]. *Corrosion*, 2002, 58 (5): 252 ~259.
- [12] Wei R P, Liao C M, Gao M. A Transmission Electron Microscopy Study of Constituent-Particle-Induced Corrosion in 7075-T6 and 2024-T3 Aluminum Alloys [J]. *Metal Mater Trans A*, 1998, 29A (1): 1 153 ~1 160.
- [13] Petroyiannis P V, Pantelakis S G. Protective role of local Al cladding against corrosion damage and hydrogen embrittlement of 2024 aluminum alloy specimens [J]. *Theoretical and Applied Fracture Mechanics*, 2005, 44 (1): 70 ~81.
- [14] Sergey N, Rashkeev. Hydrogen-Induced Initiation of Corrosion in Aluminum [J]. *J Phys Chem C*, 2007, 111 (19): 7 175 ~7 178.
- [15] El-Mahdy G A, Kim K B. AC impedance study on the atmospheric corrosion of aluminum under periodic wet dry conditions [J]. *Electrochimica Acta*, 2004, 49 (12): 1 937 ~1 948.
- [16] Szklaska-Smialowska Z. Mechanism of pit nucleation by electrical breakdown of the passive film [J]. *Corrosion Science*, 2002, 44 (5): 1 143 ~1 149.
- [17] 杨振海, 邱竹贤. 铝的电位-pH 图及铝腐蚀曲线的测定 [J]. *东北大学学报*, 2000, 21 (4): 401 ~403.
- [18] Guillaumin V, Mankowski G. Localized corrosion of 2024 T351 aluminum alloy in chloride media [J]. *Corrosion Science*, 1999, 41 (3): 421 ~438.
- [19] Posada M, Murr L E. Exfoliation and related microstructures in 2024 aluminum body skins on aging aircraft [J]. *Materials Characterization*, 1997, 38 (4, 5): 259 ~272.
- [20] Paglia C S, Buchheit R G. Microstructure, microchemistry and environmental cracking susceptibility of friction stir welded 2219-T87 [J]. *Materials Science and Engineering*, 2006, 429A (1, 2): 107 ~114.
- [21] Paglia C S, Buchheit R G. A cast 7050 friction stir weld with scandium- microstructure, corrosion and environmental assisted cracking [J]. *Materials Science and Engineering*, 2006, 424A (1, 2): 196 ~204.
- [22] 王轶农, 左 良. LY12 铝合金的再结晶织构、晶界特征分布及抗腐蚀性能 [J]. *金属学报*, 2000, 36 (10): 1 085 ~1 088. [编辑: 段金弟]

(上接第 9 页)

- [6] 范亚平, 任天斌, 黄艳霞, 等. 水性环氧树脂涂料及其固化机理的研究 [J]. *涂料工业*, 2006, 36 (7): 17 ~20.
- [7] 陈建敏, 冶银平, 党鸿辛. 粘结固体润滑膜及其应用 [J]. *摩擦学学报*, 1994, 14 (2): 180 ~189.
- [8] 周惠娣, 胡丽天, 陈建敏, 等. 一种高比压润滑涂层的研制及其摩擦学性能研究 [J]. *摩擦学学报*, 2001, 21 (5): 393 ~395.
- [9] 于 刚, 聂明德, 党鸿辛. PEP 型润滑防锈干膜的研制及其综合性能考察 [J]. *固体润滑*, 1991, 11 (2): 129 ~134.
- [10] Alex W. Chemical resistance of waterborne epoxy/amine coatings [J]. *Progress in Organic Coatings*, 1997 (32): 231 ~239.
- [11] 林 曦, 张旭东, 周 杰. II 型水性环氧体系的固化程度研究 [J]. *涂料工业*, 2007, 37 (5): 1 ~3.
- [12] Verónica Pascual-Sánchez. Influence of the curing temperature in the mechanical and thermal properties of nanosilica filled epoxy resin coating [J]. *Macromol Symp*, 2006, 233: 137 ~146.
- [13] 王月梅, 周惠娣, 陈建敏, 等. 水性粘结固体润滑涂层的摩擦学性能研究 [J]. *中国表面工程*, 2010, 23 (2): 42 ~45.
- [14] 陈建敏, 何 雪, 党鸿辛. 改性氨基四官能环氧基固体润滑涂层的研究 [J]. *固体润滑*, 1991, 11 (3): 161 ~167.
- [15] Mafi R, Mirabedini S M, Attar M M, et al. Cure characterization of epoxy and polyester clear powder coatings using differential scanning calorimetry (DSC) and dynamic mechanical thermal analysis (DMTA) [J]. *Progress in Organic Coatings*, 2005 (54): 164 ~169. [编辑: 徐 军]



Contents & Abstracts

Oxygen Evolution Electrocatalytic Performance of MnO_2 Coating Anode Electrodeposited on Titanium in Manganese Acetate Electrolyte

GAO Hong, ZHU Cheng-fei, XIE Rui, WANG Xiao-jun (College of Materials Science & Engineering, Nanjing University of Technology, Nanjing 210009, China). *Cailiao Baohu* 2010, 43 (11), 01~03 (Ch). Electrodeposited MnO_2 coatings were prepared on the surface of Ti alloy from the electrolyte consisting of MnSO_4 and the electrolyte consisting of $\text{Mn}(\text{CH}_3\text{COO})_2$ respectively. The crystal structure of the MnO_2 coatings was confirmed by means of X-ray diffraction, and the morphology was observed using a scanning electron microscope. Moreover, the electrochemical performance of the MnO_2 coating anode was evaluated based on cyclic voltammetry, polarization curve test and electrochemical impedance spectroscopy. Results show that the MnO_2 coating prepared from the electrolyte consisting of $\text{Mn}(\text{CH}_3\text{COO})_2$ has a faster deposition rate, and as-deposited Ti/ MnO_2 anode has better oxygen evolution electrocatalytic performance.

Key words: electrodeposition; MnO_2 coating; crystal structure; Ti alloy; anode; oxygen evolution electrocatalytic performance

Removal of Dissolved Aluminum in Chemical Milling Fluids by Dilute Solution Crystallization

ZHOU Guo-hua¹, FENG Qiang², YIN Mao-sheng¹, WEI Li-an² (1. Chengdu Airplane Industry Group Company Limited, China Aviation Industry Complex, Chengdu 610094, China; 2. College of Environmental and Chemical Engineering, Nanchang University of Aeronautics, Nanchang 330063, China). *Cailiao Baohu* 2010, 43 (11), 04~06 (Ch). In view of the treatment and recycle of abandoned chemical milling fluids as well as removal of dissolved Al therein, dilute solution crystallization method based on crystallization and nucleation of sodium aluminate, was adopted to remove the dissolved Al in the abandoned chemical milling fluids. The effects of dilution multiple and temperature on dissolved Al and other components were investigated. Results show that the best dilution multiple is 1.0~2.0. At 25 °C it took about 15 d to satisfactorily remove dissolved Al at a rate of about 50%~60%, while at 55 °C it took about 5~6 d to remove the dissolved Al at a rate of 30%~40%. Moreover, the content of other components such as NaOH, Na_2S and $\text{C}_6\text{H}_5\text{NO}_3$ remained unchanged after removing dissolved Al from the abandoned chemical milling fluids via dilute solution crystallization route.

Key words: chemical milling fluid; dilute solution crystallization; regeneration of chemical milling fluid; sodium aluminate; aluminum hydroxide

Influence of Curing on Physicochemical and Tribological Properties of Waterborne Epoxy Resin-Based Bonded Solid Lubricating Coatings

WANG Yue-mei^{1,2}, ZHOU Hui-di¹, CHEN Jian-min¹, CHEN Lei¹, YE Yin-ping¹ (1. State Key Laboratory of Solid Lubrication, Lanzhou Institute of Chemical Physics, Chinese Academy of Sciences, Lanzhou 730000, China; 2. Graduate University, Chinese Academy of Sciences, Beijing 100049, China). *Cailiao Baohu* 2010, 43 (11), 07~09 (Ch). An MFT-R 4000 reciprocating friction and wear tester was performed to investigate the effect of curing conditions on the tribological properties of waterborne epoxy resin-based bonded solid lubricating coatings. The optimal curing conditions were established by combining Fourier transformation infrared (FTIR) spectrometry with differential scanning calorimetry (DSC). It was found that waterborne epoxy resin-based bonded solid lubricating coatings obtained under different curing conditions possessed different tribological properties.

The optimal mass ratio of the epoxy resin emulsion to curing agent was determined to be 2:1, while the optimal curing temperature and time were suggested as 75 °C and 2 h respectively. Resultant waterborne epoxy resin-based bonded solid lubricating coating showed excellent physicochemical and tribological properties, and the antiwear life was longer than that of traditional solvent-based bonded solid lubricating coating by 30%.

Key words: solid lubricating coating; waterborne epoxy resin; bonded solid lubricant; curing condition; tribological property

Application of Stereomicroscope in Study of Corrosion of Aluminum Alloy

WANG Yu-ya^{1,2}, HAN En-hou¹ (1. Institute of Metal Research, Chinese Academy of Sciences, Shenyang 110016, China; 2. No. 10 Laboratory, Beijing Research Center of Aeronautical Technology, Beijing 100076, China). *Cailiao Baohu* 2010, 43 (11), 10~13 (Ch). With the assistance of stereomicroscopic analysis, attempts were made to realize real time observation and recurring of the corrosion process of LY12CZ Al alloy. The application of stereomicroscope in corrosion tests was explored. It was found that in EXCO solution the corrosion of Al alloy was initiated along with the destruction of surface passivation film. Corroded pits were extended along the rolling direction, which was still true even in the presence of artificial scratches perpendicular to the rolling direction. Besides, unstable colloidal $\text{Al}(\text{OH})_3$ film was able to hinder the development of local corrosion, and the regions where corrosion was initiated in preliminary stage were not necessarily to experience severe corrosion. It was feasible to realize real time observation and recurring surface corrosion process by making use of stereomicroscope and relevant technique. It is possible to more accurately study corrosion process by combining macroscopic observation with microscopic one if limits in relation to magnification times are overcome.

Key words: LY12CZ Al alloy; corrosion; stereomicroscope; macroscopic; microscopic

Formation Mechanism of Powder-Like Rust and Its Influence on Corrosion of Bronze Wares Studied by Electrochemical Methods

FENG Li-ting, SU Chang, FENG Shao-bin, LI Zhen-xing, WANG Shao-liang (Henan Provincial Key Laboratory of Surface & Interface Science, Department of Material and Chemical Engineering, Zhengzhou University of Light Industry, Zhengzhou 450002, China). *Cailiao Baohu* 2010, 43 (11), 14~16 (Ch). Several kinds of insoluble nantokite were used as active catalysts to prepare porous oxygen electrodes. Resultant porous oxygen electrodes were combined with bronze anode to produce primary batteries. The primary batteries were continuously discharged at a current density of 0.01 mA/cm² for more than 115 h, and the cathodic polarization of the porous oxygen electrodes was tested. The catalytic mechanism of the porous oxygen electrodes was discussed. It was found that the discharge test could be well used to simulate the electrochemical corrosion process of bronze wares under atmosphere. Cuprous chloride rather than basic cupric chloride was the nantokite with the highest catalytic activity for the corrosion process of bronze wares and the powder-like rust was just the final corroded product.

Key words: corrosion of bronze wares; powder-like rust; simulation of primary batteries; porous oxygen electrodes; cuprous chloride

Corrosion Inhibition Behavior of Benzotriazole for 1Cr18Ni9Ti as Nuclear Decommissioning Steel in Chemical Cleaning Agent

GONG Min¹, WEI Wei¹, ZHANG Yu¹, KANG Wu², ZHANG